IL NUOVO CIMENTO **42 C** (2019) 224
DOI 10.1393/ncc/i2019-19224-5

COMMUNICATIONS: SIF Congress 2018

# Multi-diagnostics investigation of an ECR plasma confined in a linear axis-symmetric trap

G. CASTRO

*Istituto Nazionale di Fisica Nucleare, Laboratori Nazionali del Sud - Catania, Italy*

received 15 February 2019

**Summary.** — This work presents a review of all the main methods and instruments for plasma diagnostics currently used for linear axis-symmetric plasma traps, commonly used as ion sources for accelerators and for studies of plasma physics. The simultaneous use of different diagnostics, either invasive or non-invasive, allows the characterization of the whole electron energy distribution function from a few eV to hundreds of keV. The development of space-resolved and time-resolved plasma diagnostics, moreover, is expected to further improve our knowledge of the wave-to-plasma coupling and of plasma instabilities (like the cyclotron maser), with consequences on the upgrade of existing ion sources, but also on the understanding of many astrophysical phenomena.

## 1. – Introduction

The INFN-LNS plasma team group has been working for many years on the development of an appropriate set of diagnostics tools for the investigation and characterization of plasmas generated by Electron Cyclotron Resonance Ion Sources (ECRIS) and Microwave Discharge Ion Sources (MDIS) [1]. A complete characterization of the Electron Energy Distribution Function (EEDF) would enable the improvement of the wave-to-plasma coupling, opening up new perspectives for the generation of overdense plasmas for high-intensity low-emittance ion beams. The possible capability to "shift" the EEDF towards a particular electron energy, moreover, would increase the production of the desired charge state (charge state distribution depends primarily on the EEDF [1]). Moreover, plasma is not only a source of ions to be accelerated, but also a fertile environment for studies of fundamental and applied physics [2]. Also in this perspective, the characterization of the EEDF of the plasma represents a necessary step before any subsequent study.

Figure 1 highlights the different diagnostics methods currently used for EEDF characterization: from the classical invasive measurements obtained by means of probes penetrating the plasma to non-invasive diagnostics. The latter can be divided into two

 

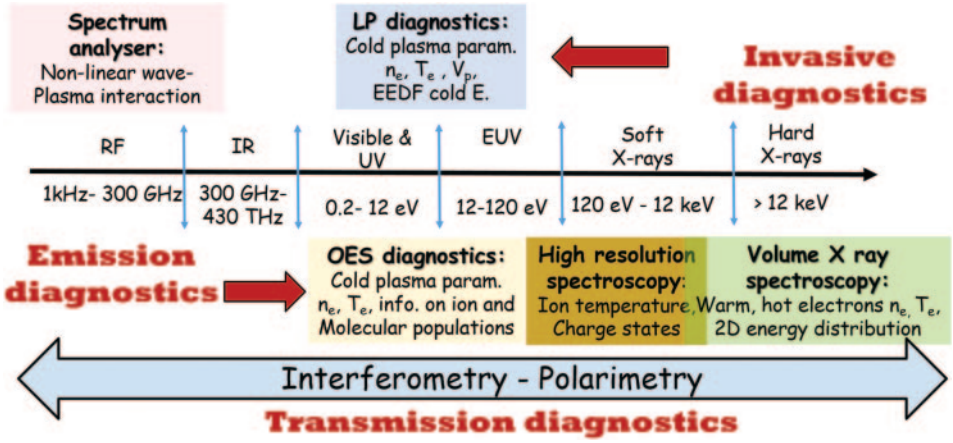


Fig. 1. – Diagnostics methods used for EEDF characterization and related electromagnetic spectrum.

sub-categories. Emission diagnostics, based on the characterization of the electromagnetic (EM) spectrum emitted by the plasma, and transmission diagnostics, which takes profit of the modification of characteristic parameters of a probing signal crossing the plasma. The simultaneous use of more diagnostics (multi-diagnostics approach) permits to characterize the whole EEDF. More and more information about plasma shape and temporal evolution can be acquired when working in space- and time-resolved mode. The development and the commissioning of these diagnostics required the design of a dedicated flexible plasma trap (FPT) [3], that was used for most of the measurements shown in this paper.

## 2. – Invasive diagnostics

The use of invasive diagnostics enables to attain local information about the properties of plasma and of the electromagnetic (EM) field propagating within the plasma chamber. This information can be obtained by means of the insertion of metal probes or small antennas within the plasma. The spatial resolution is given by the dimension of the probe or antenna, usually a few mm long and $\sim$100 $\mu$m long.

Three are the main limitations of the invasive diagnostics in ECRIS and MDIS:

1) The insertion of external devices within a compact ion source perturbs the modal behaviour of the microwaves, changing the position of the minima and maxima of the electric field and, therefore, the distribution of energetic electrons. In other words, the measuring process perturbs the results of the measurements. Recent experiments have permitted to verify that the diagnostics perturbation is lower for higher electron density plasmas: in low-density plasmas ($n_e \ll n_{cut\text{-}off}$, where $n_e$ is the electron density and $n_{cut\text{-}off}$ the microwave cut-off density), modal behaviour is dominated by the plasma chamber shape (cavity-dominated modal behaviour). However, as the plasma density increases ($n_e \geq n_{cut\text{-}off}$), the distribution of the EM wave field is dominated by the plasma distribution (plasma-dominated modal behaviour), so that the diagnostics insertion has poor influence on the measurement results [4].

2) The probe/antenna can be destroyed by the energy content of the plasma. This problem can be limited by properly setting the measurement procedure. For example, the resistivity curve should be acquired by setting the voltage to zero after any current measurement. This approach makes the acquisition time longer, but it guarantees partial cooling of the tip between two subsequent points of the resistivity curve.

3) The insertion of invasive diagnostics can cause a mismatch between microwaves and plasma chamber, leading to a decrease of the net power heating the plasma. Because of this reason, invasive diagnostics measurements should be done only in the presence of a directional coupler to verify the net power to be constant during the measurement.

**2˙1.** *Langmuir probe diagnostics.* – The Langmuir Probe (LP) diagnostics enables the evaluation of ion density, electron temperature, plasma potential and EEDF by means of the measurement of the plasma resistivity curve.

In magnetized plasmas, like those of ECRIS and MDIS, the electron component of the resistivity curve is underestimated, since the cyclotron motion limits the electron flux to the probe [5, 6]. Information about ion density can be obtained by the ion component, unaffected by the magnetic field. The electron density can be evaluated only if the mean ion charge state is known, since the quasi-neutrality condition $\langle q \rangle n_i = n_e$ ($\langle Q \rangle$ and $n_i$ being, respectively, the mean charge state and the ion density) can be applied. $\langle q \rangle$ is well known in MDIS ($\langle q \rangle = 1$), but its evaluation in ECRIS is still a challenge.

Along the years, several LP models have been developed to evaluate plasma parameters from the resistivity curve [7-11]. Their domain of validity depends on the ratio $\lambda_{Debye}/R_p$, where $\lambda_{Debye}$ is the Debye length and $R_p$ is the probe radius. Within the domain of plasma density of ECRIS ($n_e \geq 1 \cdot 10^{17}$), three LP models are currently the most suitable ones for the determination of ion density in ECRIS and MDIS [12, 13]:

1) The floating potential method, as proposed by Chen [14].

2) The orbital motion limited [7].

3) The geometric mean between the electron density determined by the Allen, Boyd and Reynold [8] model and that determined by the Bernstein, Rabinowitz and Lafambrois model [9].

The electron temperature can be properly evaluated by applying the Lafambroise approach [11] which, with an iterative procedure, is able to separate the different electron populations ($0 < T_e < 50\,\mathrm{eV}$) from the ion contribution [15].

The EEDF of the cold electrons (0–30 eV) can be estimated by means of the Druyvesteyn procedure [16]. Although the absolute values of the EEDF cannot be considered as reliable, its shape can give precious information about the plasma. For example, a double picked EEDF is a clear fingerprint of a drifting electron population within the plasma [17].

**2˙2.** *EM wave diagnostics.* – The EM spectrum can been characterized by using a movable plasma-immersed antenna, connected to a spectrum analyser for the frequency dispersive characterization. The antenna is also able to detect, together with the injected EM waves, the electrostatic (ES) waves generated by the non-linear interaction of the

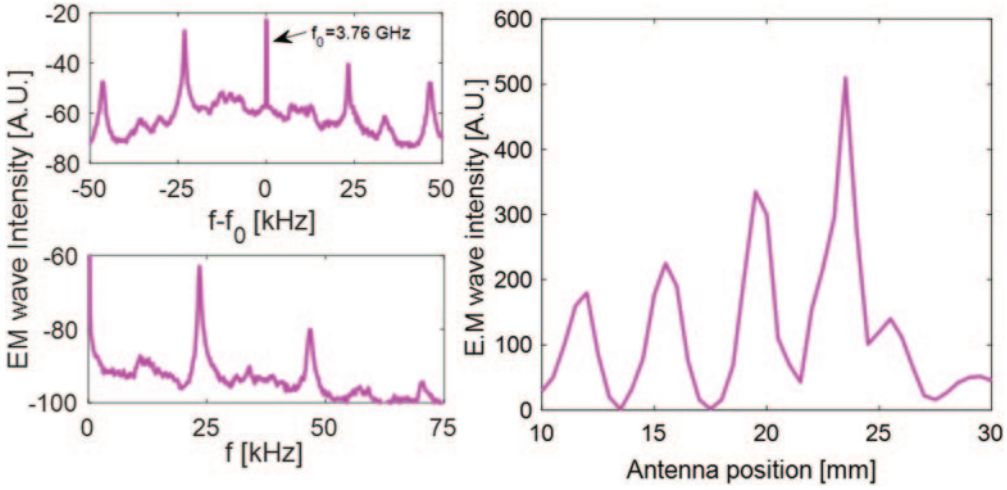


Fig. 2. – On the left, sidebands besides the 3.76 GHz pumping wave (spectrum above) are generated by the modulation instability induced by ion waves in the kHz range (spectrum below). On the right, modal behaviour characterized by means of a small antenna.

incoming EM field with plasma. The characterization of ES waves within plasma is currently one of the main hot topics in the ion source field. Several instability phenomena, as the cyclotron maser instability, are highlighted by ES wave generation. Furthermore, they are fingerprints of alternative mechanisms of plasma heating as the Electron Bernstein Wave (EBW) heating [18, 19], expected to replace/support the ECR heating for the generation of overdense plasmas [20-22]. EBW are generated by the parametric decay of the pumping wave together with a variety of ion-type waves [23]. An example of spectrum characterization is shown in fig. 2 on the left: sidebands besides the 3.76 GHz pumping wave (spectrum above) are generated by the modulation instability induced by ion waves in the kHz range (spectrum below).

If the movable antenna is connected to a RF probe diode, it is possible to characterize the EM modal behaviour, as shown in fig. 2 on the right. The coupling of the antenna to the EM field to be measured depends on the dimension of the antenna itself. Therefore, antenna dimensions can be chosen to focus onto different types of waves propagating within the plasma [4].

## 3. – Non-invasive diagnostics: The emission diagnostics

Emission diagnostics (as the optical and X-ray spectroscopy) are based on the detection of the electromagnetic radiation emitted from the plasma in different energy domains. An ECR plasma emits electromagnetic radiation in a very broad spectrum (from infrared to gamma rays), in relation to the energy of the electrons responsible of the emission. Spectroscopy techniques, therefore, provide estimates of density and temperature for specific energy populations.

**3˙1.** *Optical emission spectroscopy.* – The Optical Emission Spectroscopy (OES) technique enables a non-invasive plasma diagnostics measuring not only the electron density and temperature, but also the relative abundances of different neutral species, vibra-

tional temperature of the molecules, and concentration of the different charges states in the case of plasmas of multicharged ions.

Any line of an OES spectrum is due to a particular transition between two different atomic states of the emitting particle (ion, neutral or molecule). The line intensity is proportional to the population density of any atomic state [24].

The population densities of each state can be studied by means of three different models: the corona model, the collisional radiative (CR) model and the Boltzmann regime [24, 25]. In the density and temperature domain of ECRIS and MDIS, CR models are the most complete ones for the evaluation of plasma parameters. CR models balance all relevant population and depopulation processes for the particular states in the hydrogen atom or molecule, respectively, thereby yielding steady state population densities [24, 26]. Since CR models depend strongly on the underlying data, the quality of the results from CR models relies on the existence and quality of the cross sections (or rate coefficients). Currently, CR models are well established for atomic hydrogen, helium and argon, which are elements with clear atomic structure [27].

From an experimental point of view, the light emitted from plasma is focused, by means of a system of lenses, onto an optical fiber which leads the signal to the spectrometer. The latter resolves the spectrum with resolution $R = \lambda/\Delta\lambda$ (where $\lambda$ is the wavelength) depending on the characteristics of the instrumentation. Finally, the resolved spectrum is acquired by a CCD camera.

The spectrometer resolution is probably the most important parameter responsible for the number (and quality) of the plasma parameters valuable from measurements. A low-resolution spectrometer ($\Delta\lambda \sim 1\,\mathrm{nm}$) permits only the evaluation of electron density and temperature and, in the case of hydrogen plasmas, it enables also the evaluation of the $H/H_2$ relative abundances [28, 29]. Resolutions of the order of tens of pm enable the investigation of roto/vibrational temperature and low-charge state ion [30,31]. A further upgrade in the instrumentation resolution to a few pm enables the characterization of ion drift velocity, the splitting Zeeman, due to the effective magnetic field together with the higher charge state within the plasma [32]. Figure 3 shows, on the left, a typical hydrogen spectrum acquired with a spectrometer with resolution $R = 16000$.

**3˙2.** *X-ray spectroscopy.* – X-ray volumetric measurements enable the characterization of the electron density and temperature of plasma at medium high energy ranges. If the plasma emission is properly collimated, the determination of the plasma density is possible via the use of adequate emissivity models [33]. Silicon drift detectors are the best choice for the characterization of electron population with energy $0.5 < E < 30\,\mathrm{keV}$, while hyperpure germanium detectors should be used for the characterization of the hot electron population with $E > 30\,\mathrm{keV}$ [34]. It is to be kept in mind that plasma characterization is possible, via volume X-ray spectroscopy, only if the cone of view of the detector does not intercept the plasma chamber walls. In fact, emissivity models used for plasma parameters evaluation take into account only Bremsstrahlung cross sections of electron-ion collisions. So, electron-walls collisions may partially distort the results, especially the electron density value [35]. Typical X-ray emissivity spectra of an argon plasma, obtained during the study of the influence of the X-ray emission *vs.* the $B_{min}/B_{ECR}$ ratio ($B_{min}$ and $B_{ECR}$ being, respectively, minimum magnetic field and resonance magnetic field) are shown in fig. 3. The spectra present the $K_\alpha$ line of argon at $\sim$3 keV together with the characteristic lines of the plasma chamber at around 8 keV energy.

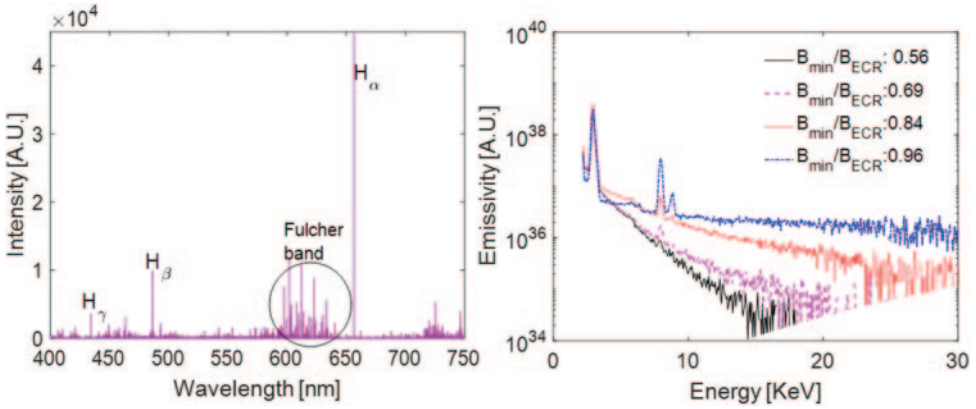


Fig. 3. – On the left, a hydrogen spectrum acquired with a spectropolarimeter with resolution $R = 16000$. On the right, typical X-ray spectra emitted by an argon plasma at different magnetic field configurations [35].

**3˙3.** *Space-resolved spectroscopy.* – Although emission spectroscopy is probably the most simple and reliable diagnostics to investigate plasma parameters, it is currently able to provide only results averaged along a cone or line of view. Because of these limitations, much effort has been made by the ion source community to develop space-resolved spectroscopy.

In the case of OES, an innovative approach was proposed in the framework of the Pandora experiment [2], borrowing from the experience acquired by the astrophysical community [36], taking advantage of the simultaneous use of three different spectropolarimeters, looking at plasma from three different points of view. The expected spatial resolution is of the order of $1\,\mathrm{mm}^3$ [32].

The X-ray space-resolved spectroscopy is being developed in these years by the common effort of the INFN-LNS and Atomki R&D ion source groups [34, 37]. 2D spatial resolution is obtained by coupling a CCD camera sensitive to the X-ray domain to a pin-hole of width of the order of a hundred $\mu$m. The so-assembled pin-hole X-ray camera guarantees spatial resolution up to $140 \times 140\,\mu\mathrm{m}^2$. More information about pin-hole camera assembling and performances can be found in ref. [38]. The pin-hole camera can be operated in two different counting modes, able to give different information about the plasma:

1) Full-count mode: the exposure time is long with respect to the X-ray emission rate (counts/s), *i.e.*, there is large probability that more than one photon strike the same pixel during single acquisition. This configuration provides valuable information on the overall structure of plasma [17, 39].

2) Photon Counting (PC) mode: In this case, any single CCD pixel is struck at most one time by X-ray photons. PC-mode operations are set by tuning appropriate exposure times of the CCD camera. The highest energy resolution $\Delta E/E$ experimentally determined was around 2% for the Fe-$K_\alpha$ [38]. In ECRIS it was possible to determine the regions where warm and colder electrons are placed (within the energy domain of the CCD) as a function of the source parameters [37] or to discriminate the displacement of the different ions inside the magnetic trap, due to the ion motion within the plasma [39].

## 4. – Non-invasive diagnostics: The transmission diagnostics

Transmission diagnostics techniques, as interferometry and polarimetry, take advantage of the modification of characteristic parameters of a probing signal when it interacts with a magnetized plasma. Characteristic parameters of the probing wave undergo modification (phase difference in the interferometric case and Faraday rotation angle in the polarimetric case) —proportionally to the plasma electronics density. Interferometry and microwave polarimetry have been fruitfully applied in large-scale fusion reactors [40] and in astrophysical plasmas, where polarimetry is a standard for either magnetic field and/or stellar density measurements [41]. The implementation of the interfero/polarimetric techniques in compact plasma traps, such as ECRIS and MDIS, is still a challenge: the main constrain consists in the small size of the plasma chamber compared to the probing wavelength. In fact, the following conditions hold: $\lambda_P \sim L_c$, being $\lambda_P$ and $L_c$ the probing signal wavelength and the plasma chamber length, respectively. That means that interference effects due to the metallic walls of the plasma chamber cannot be neglected and, in some conditions, they even prevail. In order to apply the interfero/polarimetric techniques in small plasma traps, a specific approach, based on the frequency swept method, was implemented. The frequency swept method consists in the frequency sweep of the probing signal during the interferometric/polarimetric measurement. This approach permits to remove the effects induced by multipath reflections of the probing signal within the plasma chamber [42].

**4˙1.** *Interferometry.* – The microwave interferometry determines the electron density along a line of sight by means of the frequency swept method. A beating signal is obtained by the superposition of the plasma leg signal with a reference one, while both signals sweep in time in a given frequency range. The starting value of the sweeping frequency must be greater than the cut-off frequency. As an example, in our set-up, the probing signal frequency was swept from 22.5 to 26.5 GHz, while operating at 3.75 GHz microwave frequency. By performing a fast Fourier transform analysis of the obtained beating pattern, it is possible to filter out the dominant component from the multipath contributions; hence, the beating frequency is correlated to the plasma density. Figure 4, on left, shows the frequency swept microwave interferometer block scheme according to the Mach-Zehnder scheme [42]. Further details about the experimental method can be found in ref. [43].

**4˙2.** *Polarimetry.* – The polarimetric method is based on the measurements of the so-called Faraday angle $\theta_F$ as a function of the probing wavelength $\lambda_P$. $\theta_F$ is proportional to the line integrated density $n_e$ and to $\lambda_P^2$.

The measurement of the magnetoplasma-induced rotation of the polarization plane was based on a broadband waveguide OrthoModeTransducers (OMTs) system. OMTs are inserted along the plasma leg, upstream and downstream the emitting/receiving antennas, as is shown in fig. 4, on the right.

The measurement strategy consists of transmitting the probing microwave signal from the OMT (A) inside the plasma chamber and received by the other OMT (B); the position of the OMT (B) is rotated (via in-vacuum rotatable joint connection in circular waveguide standard) in order to minimize the received power on the cross-polar port of the OMT (B) itself [44].

The interfero/polarimetric techniques were tested and commissioned for the first time in a compact ion source in 2017/2018 by using the same experimental set-up already

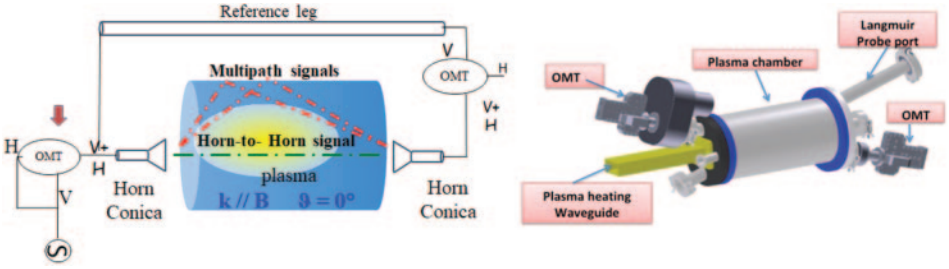


Fig. 4. – On the left, the set-up for interferometry. On the right, the set-up for polarimetry.

described in refs. [17, 42]. The interferometric technique estimated a density equals to $n_e = (2.1 \pm 0.4) \cdot 10^{18}\,\mathrm{m}^{-3}$, while the polarimetric technique estimated $n_e = (2.9 \pm 0.8) \cdot 10^{18}\,\mathrm{m}^{-3}$ [45]. The mutual agreement between the two values can be considered as a validation of the experimental approach.

## 5. – Time-resolved diagnostics

The diagnostics described in previous sections are able to give important information about the steady state plasma characteristics. Plasma parameters are averaged within the measurement time. For example, the LP resistivity curve and OES spectra are acquired in hundreds of ms, while X-ray spectra acquisition can require up to hundreds of seconds. Unfortunately, several phenomena occurring in plasma are characterized by time-scale lower than ms.

The study of the first and last instants of the plasma life has huge importance in plasma research. In proton sources, for example, the first reactions favour the generation of a $H_2^+$-rich plasma. The ionized molecules, however, are broken up into protons in some ms by plasma electrons to generate a proton-rich plasma [46]. The recent interest of the accelerator community for $H_2^+$ ion sources [47-49], consequently, increased the importance of the experimental characterization of the first tens of $\mu$s of the hydrogen plasma life.

After-glow discharge of highly charged ions from ECRIS is another well-known phenomenon that requires time-resolved diagnostics to be fully investigated. The rise time of discharge is of the order of $\mu$s, while fall time is of the order of ms [50].

Moreover, recent studies put in evidence the existence of instability phenomena, known as Cyclotron Maser (CM) instabilities that have destructive effects on the plasma stability and ion confinement. With a time-scale of the order of ns, CM instability leads to a sudden de-confinement of plasma electrons and the subsequent emission of burst of microwaves and X-rays [51, 52].

The investigation and characterization of all these phenomena requires a complete set of *ad hoc* diagnostics, which is being developed at INFN-LNS. Time-resolved measurement requires the use of oscilloscopes characterized by high sample rate and frequency to have the maximum temporal resolution. New-generation oscilloscopes also permit time-resolved spectral analysis, thus enabling the simultaneous temporal investigation of EM and ES waves propagating within the plasma.

For the correct investigation of low time-scale plasma phenomena, the oscilloscope should be accurately triggered. For the study of plasma ignition or after-glow, trigger signal can be given, respectively, by switching on and off the microwave generator. Much more difficult is the choice of the trigger system for plasma instability characterization.

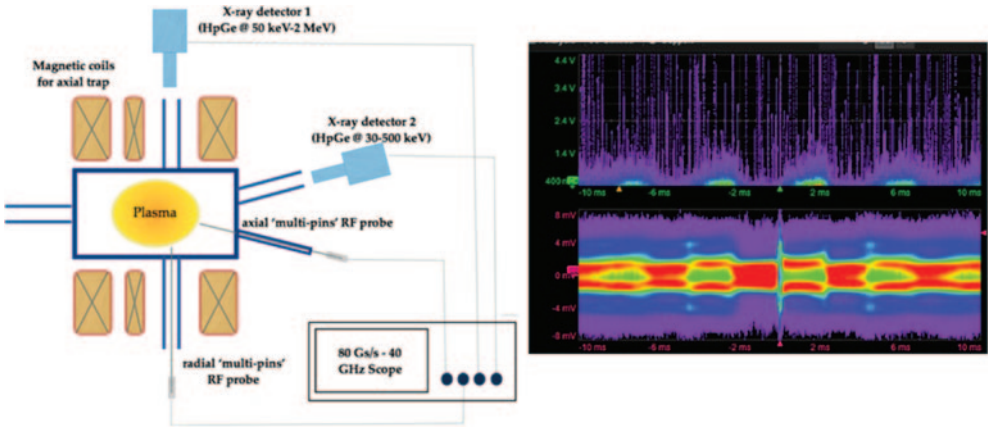


Fig. 5. – On the left, experimental set-up used for measurements of time-resolved spectroscopy. On the right, time-resolved X-ray spectrum and EM spectrum detecting CM instability in the plasma trap experimental set-up.

In most of the cases, one would trigger the instability itself. To clarify this concept, the set-up for the time-resolved investigation of CM instability at INFN-LNS, together with a typical time-resolved spectrum, is shown in fig. 5. An 80 Gs/s 40 GHz oscilloscope is connected to two different X-ray detectors and two multi-pins RF probes [4] (fig. 5 on the left). Once the CM instability was excited [35], the cyclotron emission detected by the RF probes was used as oscilloscope trigger. Figure 5 on the right shows preliminary experimental results: strong X-ray emission, with pulses of the order of ms (spectrum above) is generated in coincidence with the plasma self-emission of sub-harmonics of the pumping wave, *i.e.*, cyclotron waves (spectrum below). Details of the technique and first results have been published in ref. [53].

* * *

The contribution of all members of the plasma physics and ion source team of the INFN-LNS has been essential for the present work.

REFERENCES

[1] Geller R., *Electron Cyclotron Resonance Ion Sources and ECR Plasmas* (IOP, Bristol) 1996.
[2] Mascali D. *et al.*, *Eur. Phys. J. A*, **53** (2017) 7.
[3] Gammino S. *et al.*, *J. Instrum.*, **12** (2017) P07027.
[4] Torrisi G. *et al.*, *IEEE Trans. Antennas Propag.*, **67** (2018) 2142.
[5] Brussaard G. J. H. *et al.*, *Phys. Rev. E*, **54** (1996) 1906.
[6] Bon-Woong Koo *et al.*, *J. Appl. Phys.*, **86** (2018) 1213.
[7] Mott-Smith M. and Langmuir I., *Phys. Rev.*, **28** (1928) 727.
[8] Allen J. E., Boyd R. L. F. and Reynolds P., *Proc. Phys. Soc. London B*, **70** (1957) 297.
[9] Bernstein B. and Rabinowitz I. N., *Phys. Fluids*, **2** (1959) 112.
[10] Lam H., *Phys. Fluids*, **8** (1965) 73.
[11] Godard R. and Lafambroise J. G., *Planet. Space Sci.*, **31** (1983) 275.
[12] Chen F. F., *Plasma Sources Sci. Technol.*, **21** (2012) 055002.

[13] Chen F. F., *Plasma Sources Sci. Technol.*, **18** (2009) 035012.
[14] Chen F. F. *et al.*, *Phys. Plasmas*, **9** (2002) 1449.
[15] Chen F. F. *et al.*, *Phys. Plasmas*, **8** (2001) 3029.
[16] Druyvesteyn M. J., *Z. Phys.*, **64** (1930) 781.
[17] Castro G. *et al.*, *Plasma Sources Sci. Technol.*, **26** (2017) 055019.
[18] Berstein I. B., *Phys. Rev.*, **109** (1958) 10.
[19] Golovanivsky K. S. *et al.*, *Phys. Rev. E*, **52** (1995) 255003.
[20] Podoba Y. Y. *et al.*, *Phys. Rev. Lett.*, **98** (2007) 10.
[21] Preinhaelter J., *Plasma Phys. Control. Fusion.*, **51** (2009) 125008.
[22] Castro G. *et al.*, *Rev. Sci. Instrum.*, **83** (2012) 02B501.
[23] Castro G. *et al.*, *Rev. Sci. Instrum.*, **87** (2016) 02A507.
[24] Fantz U., *Plasma Sources Sci. Technol.*, **15** (2006) S137.
[25] Griem H. R., *Principles of Plasma Spectroscopy* (Cambridge University Press, Cambridge) 1997.
[26] Fantz U. *et al.*, *Nucl. Fusion*, **46** (2006) S297.
[27] Wunderlich D. and Fantz U., *Atoms*, **4** (2016) 26.
[28] Wu W. B. *et al.*, *AIP Conf. Proc.*, **2011** (2018) 020004.
[29] Mazzaglia M. *et al.*, *Phys. Rev. Accel. Beams*, **22** (2019) 053401.
[30] Briefi S. *et al.*, *J. Quant. Spectrosc. Radiat. Transf.*, **187** (2017) 135.
[31] Kronholm R. *et al.*, *Rev. Sci. Instrum.*, **89** (2018) 043506.
[32] Giarrusso M. *et al.*, *J. Instrum.*, **13** (2018) C11020.
[33] Gumberidze A. *et al.*, *Rev. Sci. Instrum.*, **81** (2010) 033303.
[34] Mascali D. *et al.*, *Rev. Sci. Instrum.*, **87** (2016) 02A510.
[35] Miracoli R. *et al.*, *J. Instrum.*, **14** (2019) C01016.
[36] Fleishman G. D. *et al.*, *Astrophys. J.*, **839** (2017) 30.
[37] Racz R. *et al.*, *Plasma Sources Sci. Technol.*, **26** (2017) 075011.
[38] Romano F. P. *et al.*, *Anal. Chem.*, **86** (2014) 10892.
[39] Mascali D. *et al.*, *J. Instrum.*, **12** (2017) C12047.
[40] Scime E. E. *et al.*, *Rev. Sci. Instrum.*, **72** (2001) 1672.
[41] Ramkumar P. S. and Deshpande A. A., *J. Astrophys. Astron.*, **20** (1999) 37.
[42] Torrisi G. *et al.*, *Rev. Sci. Instrum.*, **87** (2016) 02B909.
[43] Mascali D. *et al.*, *Rev. Sci. Instrum.*, **87** (2016) 095109.
[44] Torrisi G. *et al.*, *J. Instrum.*, **12** (2017) C10003.
[45] Naselli E. *et al.*, *J. Instrum.*, **12** (2018) C12020.
[46] Xu Y. *et al.*, *Rev. Sci. Instrum.*, **85** (2014) 02A943.
[47] Alonso J. *et al.*, *J. Instrum.*, **10** (2015) T10003.
[48] D'Agostino G., *Nuovo Cimento C*, **41** (2018) 120.
[49] Castro G. *et al.*, *Rev. Sci. Instrum.*, **87** (2016) 083303.
[50] Langbein K., *Rev. Sci. Instrum.*, **67** (1996) 1334.
[51] Izotov I. *et al.*, *Plasma Sources Sci. Technol.*, **24** (2015) 045017.
[52] Skalyga V. *et al.*, *Phys. Plasmas*, **22** (2015) 083509.
[53] G. Castro *et al.*, *J. Instrum.*, **14** (2019) C10035.